A time reversal damage imaging method for structure health monitoring using Lamb waves*

Zhang Hai-Yan(张海燕)†, Cao Ya-Ping(曹亚萍), Sun Xiu-Li(孙修立), Chen Xian-Hua(陈先华), and Yu Jian-Bo(于建波)

School of Communication and Information Engineering, Key Laboratory of Specialty Fiber Optics and Optical Access Networks, Shanghai University, Shanghai 200072, *China*

(Received 26 March 2010; revised manuscript received 23 April 2010)

This paper investigates the Lamb wave imaging method combining time reversal for health monitoring of a metallic plate structure. The temporal focusing effect of the time reversal Lamb waves is investigated theoretically. It demonstrates that the focusing effect is related to the frequency dependency of the time reversal operation. Numerical simulations are conducted to study the time reversal behaviour of Lamb wave modes under broadband and narrowband excitations. The results show that the reconstructed time reversed wave exhibits close similarity to the reversed narrowband tone burst signal validating the theoretical model. To enhance the similarity, the cycle number of the excited signal should be increased. Experiments combining finite element model are then conducted to study the imaging method in the presence of damage like hole in the plate structure. In this work, the time reversal technique is used for the recompression of Lamb wave signals. Damage imaging results with time reversal using broadband and narrowband excitations are compared to those without time reversal. It suggests that the narrowband excitation combined time reversal can locate and determine the size of structural damage more precisely, but the cycle number of the excited signal should be chosen reasonably.

Keywords: Lamb wave, time reversal, damage imaging, structure health monitoring
PACC: 4320, 4335, 4735

1. Introduction

The use of Lamb waves for structural health monitoring has attracted increased attention in recent years.[1−4] Conventional ultrasonic inspections are point-by-point scanning with bulk waves generated and received at normal incidence, which takes a lot of time for large structures. Lamb wave inspection are often the preferred candidate of acoustic wave modes for the inspection of large plate-like structures because they can be excited at one point of a structure and can be propagated over considerable distances. Hence, a relatively large area of the structure can be interrogated between actuator and sensor.[5] However, Lamb wave inspection is not a well-established technique.[6] The key problems for data interpretation are the existence of at least two Lamb wave modes with dispersive nature and the generation of new Lamb wave modes by mode conversion at damages. Although one may excite only one specific mode for the inspection, the presence of many conversion modes is inevitable after the interaction with a defect. These modes will share the energy and hence depress the signal to noise ratio.[7] If one tries to enhance the inspection energy by increasing the cycles of excited signals, which will make the wave packet broaden when the exciting frequency is invariant, the dispersive characteristic of this broadened wave will cause difficulties of identifying the defect echo. Hence, one new approach is required to reduce the dispersion effects of Lamb waves. One such method is the time reversal method.

The concept of time reversal has been studied in many contexts including ultrasonic imaging,[8,9] nondestructive testing,[10,11] and wireless communications.[12] Núñez and Negreira[13] have developed a theoretical background for the interpretation of the time reversal processes applied to the refocalisation of acoustic waves in dispersive media with multimode propagation of waves. It is demonstrated that the signal recompression enhances when the medium is highly dispersive and when there are several modes involved in the process. Recently, time reversal recompression has been verified to be effective for the dispersed multimode Lamb wave signals.[14]

*Project supported by the National Natural Science Foundation of China (Grant Nos. 10874110 and 10504020), Shanghai Leading Academic Discipline Project, China (Grant No. S30108) and Science and Technology Commission of Shanghai Municipality, China (Grant No. 08DZ2231100).
†Corresponding author. E-mail: hyzh@shu.edu.cn
© 2010 Chinese Physical Society and IOP Publishing Ltd

The following papers present different uses of time reversal Lamb waves for damage detection.

Gangadharan *et al.*[15] investigated time reversal active sensing by using Lamb waves for health monitoring of a metallic structure. Experiments were performed on aluminum plates to show that broadband excitation combining with time reversal is more suitable in resolving and detecting defects located near to each other in comparison with tone burst signal excitation. Experiments were also performed to show that broadband pulse along with time reversal was effective enough in reducing the dispersion effect of Lamb waves and enhancing the signal to noise ratio. Xu and Giurgiutiu[16] developed a theoretical model for predicting the single mode tuning effects on Lamb wave time reversal with piezoelectric wafer active sensors for structural health monitoring. The validity of the proposed theoretical model was verified through experimental studies. The advantages of single mode tuning in the application of time reversal damage detection were highlighted. Sohn *et al.*[17] proposed an enhanced time reversal method to assess damage in composite plates. They developed wavelet-based signal processing techniques to enhance the time reversibility of Lamb waves. The time reversibility was violated when nonlinearity is caused by a defect along a direct wave path. Examining the deviation of the reconstructed signal from the known initial input signal allowed instantaneous identification of damage without requiring the baseline signal for comparison. The validity of the proposed method was exemplified through experimental studies on a quasi-isotropic laminate with delamination. Park *et al.*[18] demonstrated the applicability of time reversal Lamb waves to improve the detectability of local defects in composite plate structures. They developed a reference-free damage diagnosis technique based on the time reversal process so that defects could be identified without relying on any past baseline data. Wang *et al.*[8] proposed a synthetic time reversal arrays method as an effective means of improving the signal to noise ratio of *in situ* monitoring systems and an imaging method for locating and approximate sizing of structural damages.

In this paper, a time reversal Lamb wave damage imaging method is investigated in an aluminum plate structure. Numerical simulations based on a finite element model are conducted to study the time reversal behaviour of Lamb wave modes under broadband and narrowband excitations. Experiments combining finite element model are then conducted to study the imaging method in the presence of damage like hole in the plate structure. In this work, the time reversal technique is used for the recompression of Lamb wave signals. Damage imaging results with time reversal using broadband and narrowband excitations are compared to those without time reversal. It is suggested that the narrowband excitation combined time reversal can locate and determine the size of structural damage more precisely, but the cycle number of the excitation signal should be chosen reasonably.

2. Lamb wave time reversal

2.1. Time reversal principle

In the time reversal procedure, an input signal can be reconstructed at the excitation point if an output signal recorded at another point is reversed in time domain and emitted back to the original source point. Consider two piezoelectric transducers (PZTs), denoted as A and B, at distance r apart. Taking no account of the electro-mechanical and mechanical-electro efficiencies of PZTs, we first apply an excitation $V_{\rm A}(\omega)$ to transducer A and the corresponding response $V_{\rm B}(\omega)$ at transducer B, $V_{\rm A}(\omega)$ and $V_{\rm B}(\omega)$ are related the following equation:

$$V_{\rm B}(\omega) = G(\omega) V_{\rm A}(\omega), \tag{1}$$

where $G(\omega)$ is the frequency-dependent structure transducer function that affects the wave propagation through the medium. In the second step, the response $V_{\rm B}(\omega)$ is reversed in the time domain and is applied back to transducer B. Note that the time reversal operation of a signal in the time domain is equivalent to taking the complex conjugate of the Fourier transform of the signal in the frequency domain. In the final step, the reconstructed signal $V_{\rm R}(\omega)$ at transducer A can be obtained by reemitting the time reversed version of $V_{\rm B}(\omega)$ at transducer B. The $V_{\rm R}(\omega)$ can be related to the $V_{\rm B}(\omega)$ in the previous step as follows:

$$V_{\rm R}(\omega) = G(\omega) V_{\rm B}^{*}(\omega), \tag{2}$$

where the superscript * denotes the complex conjugate operation. The transfer function $G(\omega)$ in Eq. (2) is assumed to be identical to the one in Eq. (1) based on the reciprocity of elastodynamics.[19] By inserting Eq. (1) into Eq. (2), the reconstructed signal, $V_{\rm R}(\omega)$, is related to the original input signal, $V_{\rm A}(\omega)$,

$$\begin{aligned} V_{\rm R}(\omega) &= G(\omega) V_{\rm B}^{*}(\omega) = G(\omega) G^{*}(\omega) V_{\rm A}^{*}(\omega) \\ &= |G(\omega)|^{2} V_{\rm A}^{*}(\omega). \end{aligned} \tag{3}$$

The above Eq. (3) indicates that the reconstructed wave $V_{\mathrm{R}}(\omega)$ has the same phase spectrum as the excitation $V_{\mathrm{A}}(\omega)$, while its magnitude spectrum is modulated by the frequency-dependent time reversal operation $|G(\omega)|^2$. The original input signal cannot be properly reconstructed if the input signal consists of multiple frequency components such as a broadband input signal. To avoid this issue, a narrowband excitation should be used. In order to verify the above theoretical results, numerical simulations are performed for both broadband and narrowband excitations which will be discussed in the next section.

2.2. Time reversal validation

To justify the use of broadband and narrowband excitation for the time reversal process, numerical simulations are conducted on an aluminum plate model using the commercial finite element software ANSYS 11. The geometric configuration of the aluminum plate and the location of transducers are properly arranged as shown in Fig. 1 so that only the A_0 mode is generated when transducers A and D are excited simultaneously.[14] The polarisation of transducers B and C is configured to be identical to that of transducers A and D. Reversing and reemitting the response signal at transducers B and C in the time domain, reconstructed input signals are received at transducers A and D. The sheet thickness of transducer is 0.127 mm. The 1-cycle, 5-cycle and 10-cycle tone burst input signals shown in Figs. 2(a), 3(a) and 4(a) respectively at a frequency of 200 kHz are employed to numerically simulate the time reversal process.

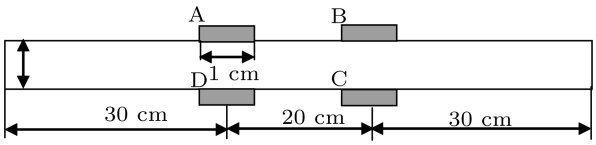


Fig. 1. An aluminum plate model with two pairs of surface-bonded PZT transducers to generate single mode Lamb wave.

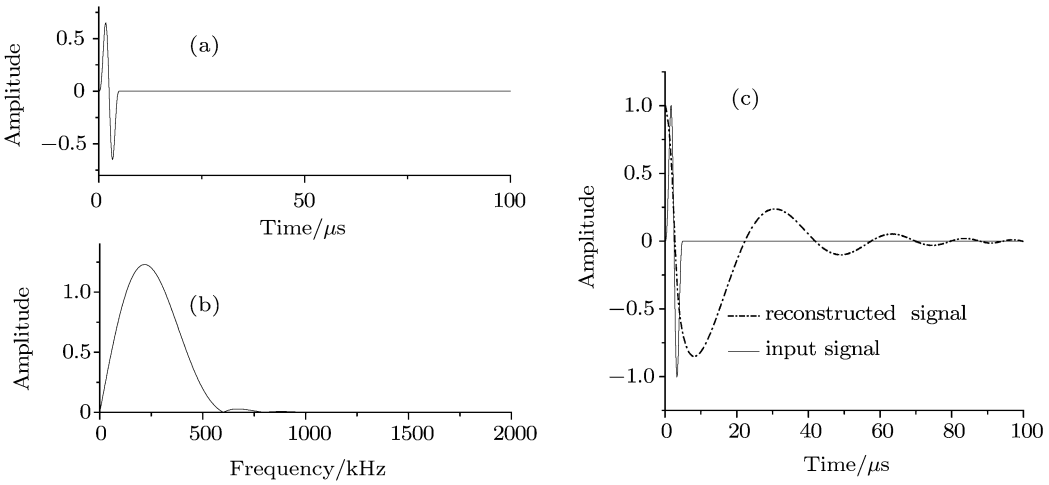


Fig. 2. The 1-cycle tone burst: (a) time sequence; (b) Fourier transform and (c) reconstructed signal.

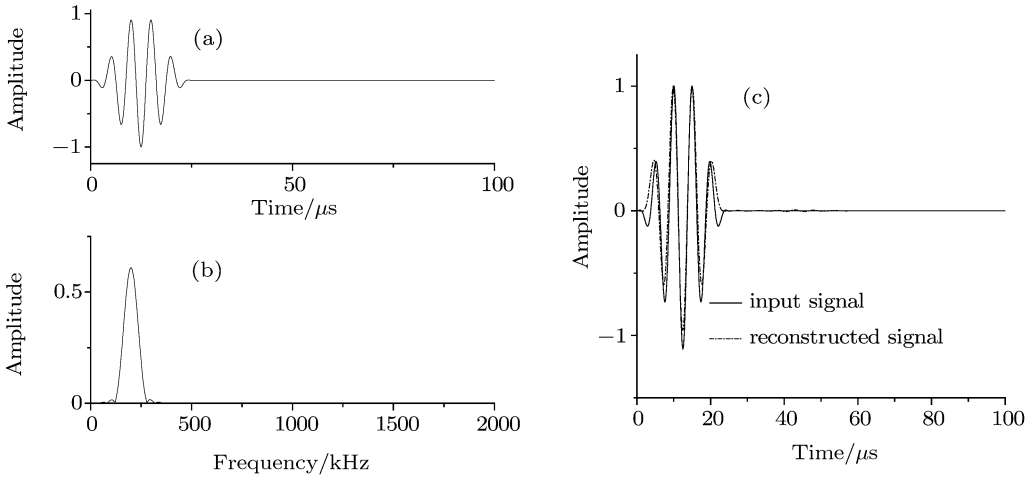


Fig. 3. The 5-cycle tone burst: (a) time sequence; (b) Fourier transform and (c) reconstructed signal.

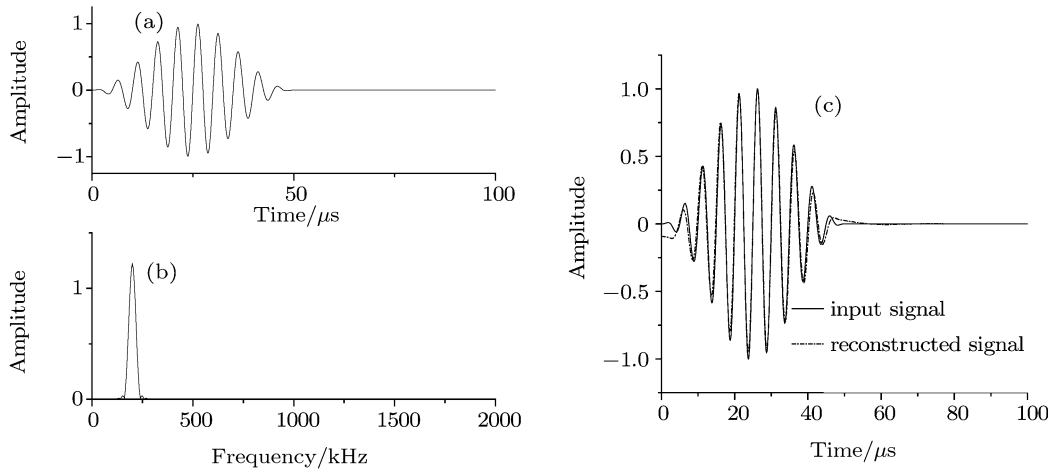


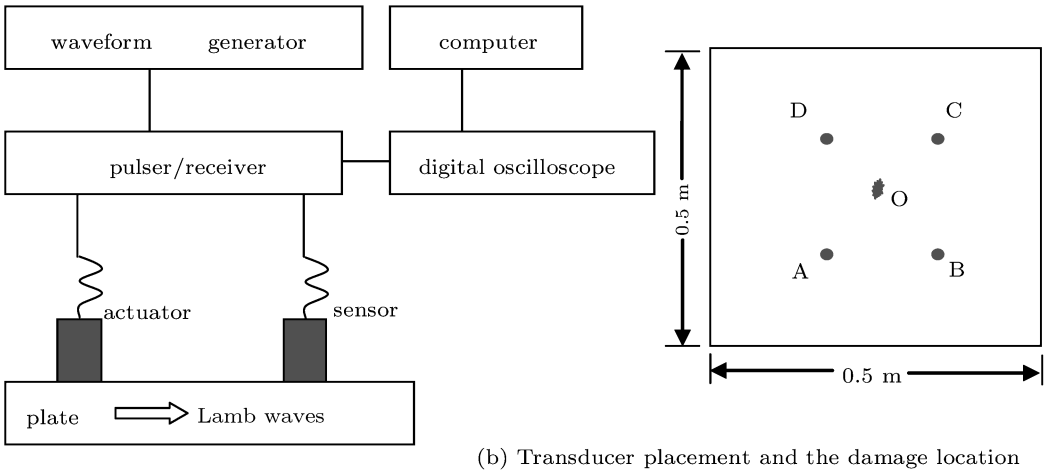
Fig. 4. The 10-cycle tone burst: (a) time sequence; (b) Fourier transform and (c) reconstructed signal.

The original input and the reconstructed input signals are demonstrated in Figs. 2(c), 3(c) and 4(c) respectively. As observed here, the reconstructed input signals are more precisely close to the original input signals with the increase of the number of cycles. This is because the signal energy is more concentrated on the central frequency when more cycle number is used, as shown in Figs. 2(b), 3(b) and 4(b).

3. Structural damage imaging

3.1. Experimental setup

The experimental setup is illustrated in Fig. 5(a). Tone burst signals from a Agilent 33250A arbitrary waveform generator were amplified and filtered by using a Panamatrics 5073PR pulser/receiver and used to drive a 200 kHz PZT. Lamb wave signals were obtained with Tektronix DPO4032 digital oscilloscope and saved into a computer by general purpose interface bus GPIB. The schematic diagram of the aluminum specimen with the four identical PZT sensors is shown in Fig. 5(b). The dimensions of the specimen are 500×500×4 mm^3. Damage was introduced into the plate by drilling a hole into the centre of the plate. The coordinates of the four transducers and hole are A(-100,-100), B(100,-100), C(100,100), D(-100,100),O(0,0), respectively, and the unit is mm. The thickness and diameter of the PZT used are 0.127 mm and 27 mm, respectively. The hole diameter is 10 mm.



(a) Experimental diagram

(b) Transducer placement and the damage location

Fig. 5. Schematic diagram of the experimental setup and the aluminium specimen with four transducers and a hole damage.

Experiment was first conducted to excite single Lamb wave mode to avoid the multimodal effect which makes it difficult to analyse and interpret the experimental signals. A Hanning-windowed 5-cycle tone burst signal centred at 200 kHz was used for exciting the transducer A and the amplitudes of S_0 and A_0 modes were picked by the transducer B. The experimental signal is shown in Fig. 6. At this frequency, A_0 mode wave is significant while S_0 mode waves carry less energy which can be neglected. By computation, the velocity of the A_0 mode in the experiment is 3018 m/s, which is coincidental with its theoretical group velocity 2998 m/s.

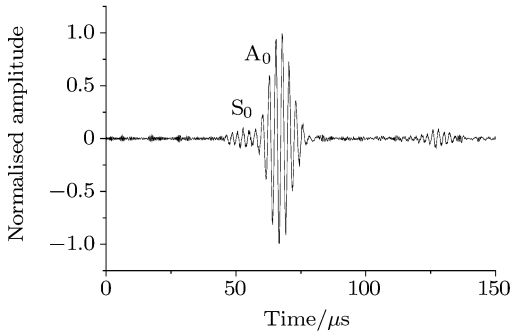


Fig. 6. Normalised transducer response at transducer B when transducer A is excited by a Hanning-windowed 5-cycle tone burst.

In Lamb active health monitoring technology, if there is damage in a sample plate, then an acoustic wave launched from an active source such as a PZT will be reflected by the damage, which acts as a passive source. If the response of the PZT to the acoustic wave with and without the damage is stored respectively and then subtracted one from the other, the difference will be the signal due to the presence of the damage, which is referred as scattered signal emanating from the damage location and can be further used to image. The imaging method in this study can be divided into two steps. A coarse image can be first constructed using the scattered signals received by all the sensors in the network. From this coarse image, approximate location of structural damage can be found. Then a refined image can be generated by using a time reversal damage imaging method described in Refs. [8] and [9]. The imaging algorithm used in this study is expressed as

$$S(x,y)=\prod_{i=1}^{N}\prod_{j=1}^{N}A_{ij}f_{ij}^{(s)}\left(\frac{R_i+R_j}{V_{\rm g}}\right), \qquad (4)$$

where $f_{ij}^{(s)}(t)$ denotes the received scattered signal by sensor j due to the excitation of sensor i. The R_i and R_j denote respectively the distances between sensors i and j and the imaging pixel (x,y). The parameter $V_{\rm g}$ denotes the group velocity of the Lamb wave signal in the structure, which is 3018 m/s in this study. The A_{ij} is the amplification coefficient for compensating the energy attenuation of each sensor pair, which is uniformly equal to 2.54×10^{10} in following imaging for simplicity.

3.2. Experimental results

To simplify data analysis, four transducers were placed symmetrically around the hole. Two experiments were performed, one on the specimen without hole and one on the specimen with the hole. In each experiment, one transducer was employed as the actuator while the other three were employed as sensors. Subtraction of the latter from the former response yielded the scattered wave due to the hole. According to reciprocal theory for an infinite media[19] and the symmetry of the transducers about the hole, there were only two independent scattered signals in the present case. As an example, scattered responses at transducers B, C when transducer A was excited with 1-cycle tone burst of 200 kHz central frequency are shown in Fig. 7. A coarse image can be constructed by using the scattered signals in Fig. 9(a) below. The four transducers are highlighted by the white dots while the black dash circle indicates the actual location and size of the damage. It can be seen that ultrasonic energy decentralizes around the damage. The damage can be further identified and located more precisely based on a finite element numerical model.

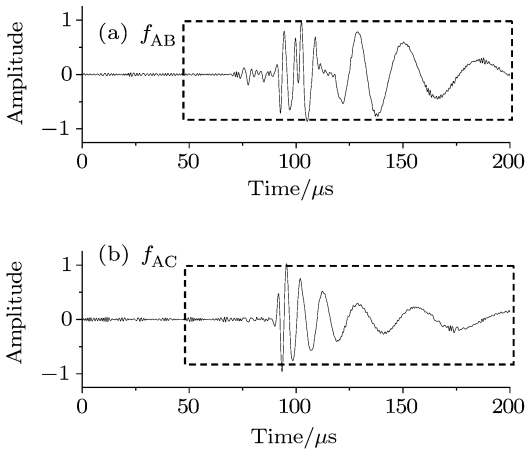


Fig. 7. Scattered responses at (a) transducer B, (b) transducer C.

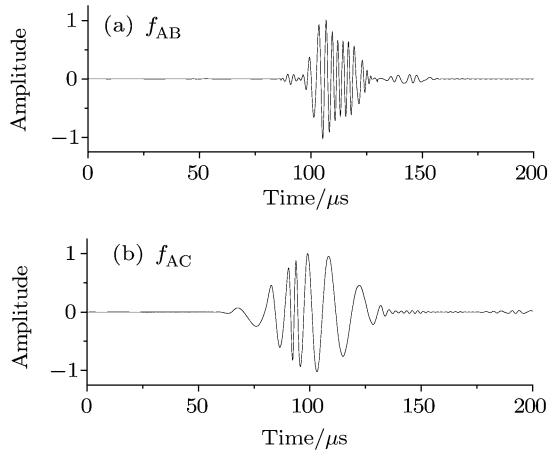


Fig. 8. Time reversed response at (a) transducer B and (b) transducer C.

For the signal shown in Fig. 7, a rectangular window with the length 154 μs (designated with dashed block) was chosen to retain only the reflected signal from the damage to each transducer and removed the transmitted signal from the actuator to the damage. Intercepted signals were then time reversed and actuated at approximate damage location. Time reversed waves propagating in a simulating plate without the hole were picked up by the sensors A, B, C and D based on the finite element model. Figure 8 displays the received Lamb wave signals for both the cases shown the Fig. 7, which clearly shows the temporal recompression of dispersive Lamb waves. Signals of Fig. 8 were applied to the Eq. (4), the imaging results are shown in Fig. 9(b). It has been observed that the ultrasonic energy converges to the damage more intensively than that in Fig. 9(a).

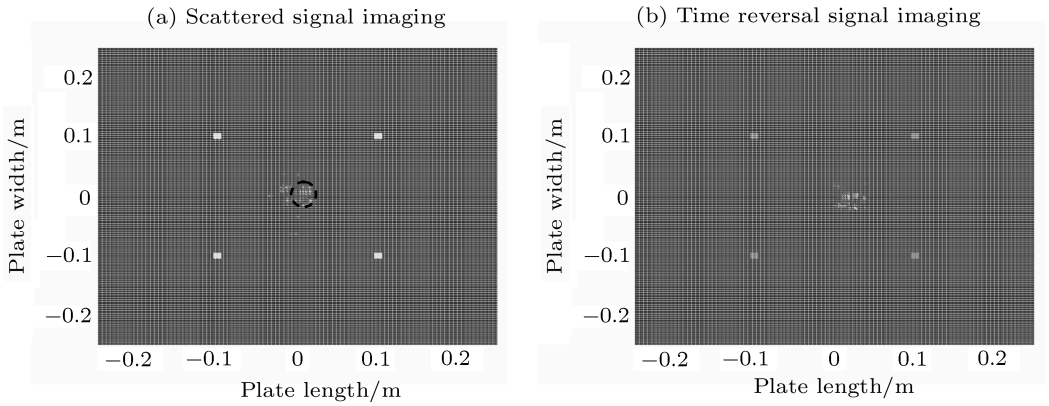


Fig. 9. Image obtained from 1-cycle tone burst excitation at 200 kHz central frequency.

The procedure discussed above for 1-cycle tone burst was repeated for 5-cycle and 10-cycle cases, respectively, shown in Figs. 10 and 11. As expected, images with time reversal locate and determine the size of structural damage more precisely compared to those without time reversal.

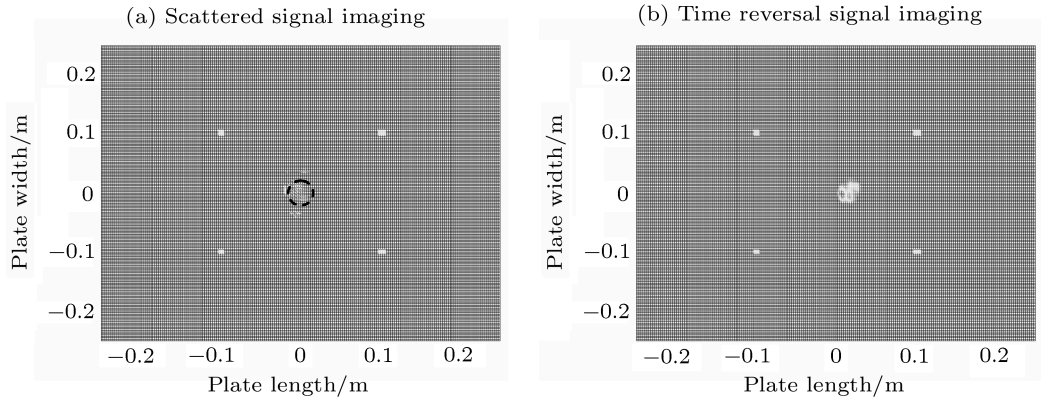


Fig. 10. Image obtained from 5-ycle tone burst excitation at 200 kHz central frequency.

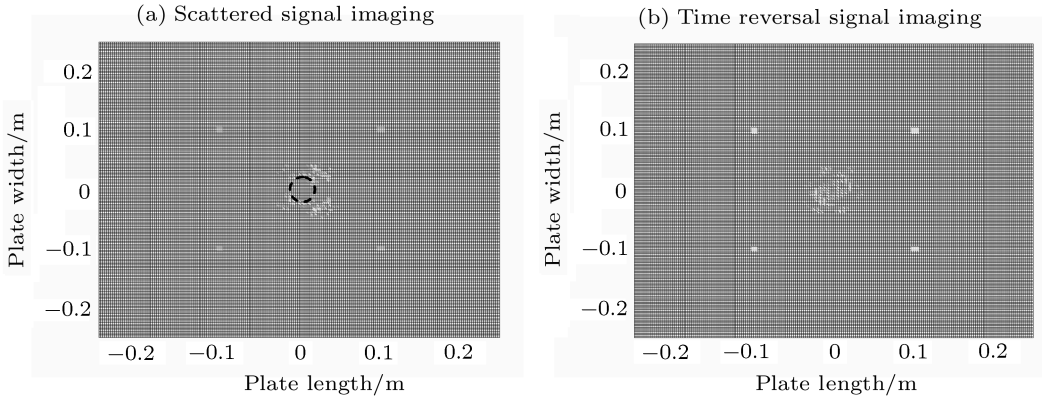


Fig. 11. Image obtained from 10-cycle tone burst excitation at 200 kHz central frequency.

In this study, a sine tone burst wave modulated by the Hanning window was used as the input signal. For a tone burst excitation at a central frequency, the signal energy is more concentrated on the central frequency with the increase of the number of cycles. Attributing to the frequency dependency of the time reversal operation described in Section 2, the temporal focusing effect of the time reversed Lamb wave is a function of cycles at specified exciting frequency and Lamb wave mode. To yield stronger scattered signal, tone burst number of cycles should be increased. However, resolution of damage under narrowband excitation is not a function of the number of cycles. As observed in Figs. 10(b) and 11(b), the image obtained from 5-ycle tone burst excitation gives the higher resolution for determining the location and size of damage. This is because the signal bandwidth is inversely proportional to the signal time duration. Since the amplitude of scattered wave is used to construct an image for the damage, the increase of cycle number will make the wave packet broaden, which results in the enlarging imaging region. To gain higher resolution for identifying the damage, the tone burst number of cycles should be chosen reasonably.

4. Conclusions

Lamb wave imaging method combining time reversal is investigated for health monitoring of a metallic plate structure. The temporal focusing effect of the time reversal Lamb waves is investigated theoretically and verified by numerical examples. Experiments combining finite element model are conducted to study the imaging method in the presence of damage like hole in the plate structure. Damage imaging results with time reversal using broadband and narrowband excitations are compared to those without time reversal. Important conclusions drawn from the current research are as follows.

(a) The temporal focusing effect of the time reversal Lamb waves can be used to enhance the inspection energy in structural damage imaging.

(b) Frequency dependence of time reversal operation implies that the narrowband tone burst signal should be excited. Generally, the more the cycle number, the better the focusing effect.

(c) Structural damage imaging combined time reversal can locate and determine the size of damage more precisely compared to those without time reversal.

(d) It is the amplitude that stands for the strength of scattered wave is used to construct an image of a scatter (damage) in this paper. Under the invariant exciting frequency and Lamb wave mode, the increase of cycle number will make the wave packet broaden, which results in the enlarging imaging region. To gain higher resolution for identifying the damage, the tone burst number of cycles should be chosen reasonably.

References

[1] Li F C and Meng G 2008 *Acta Phys. Sin.* **57** 4265 (in Chinese)

[2] Zhang H Y, Liu Z Q and Ma X S 2003 *Acta Phys. Sin.* **52** 2492 (in Chinese)

[3] Xiang Y X and Deng M X 2008 *Chin. Phys.* B **17** 4232

[4] Zhang R, Wan M X and Cao W W 2000 *Acta Phys. Sin.* **49** 1297 (in Chinese)

[5] Betz D C, Thursby G, Culshaw B and Staszewski W J 2003 *Smart Mater. Struct.* **12** 122
[6] Li F C, Meng G, Ye L, Ye L and Kageyama K 2009 *Meas. Sci. Technol.* **20** (http://iopsicence.iop.org/0957-0233/20/9/095704)
[7] Deng F, Wu B and He C F 2008 *J. Pressure Vessel Technol.* **130** 021503-1
[8] Wang C H, Rose J and Chang F K 2004 *Smart Mater. Struct.* **13** 415
[9] Zhang H Y, Sun X L, Cao Y P, Chen X H and Yu J B 2010 *Acta Phys. Sin.* **59** (in Chinese)
[10] Butėnas G and Kažys R 2006 *Ultragarsas* **61** 34
[11] Butėnas G and Kažys R 2007 *Ultragarsas* **62** 38
[12] Ge G D, Wang B Z, Huang H Y and Zheng G 2009 *Acta Phys. Sin.* **58** 8249 (in Chinese)
[13] Núñez I and Negreira C 2005 *J. Acoust. Soc. Am.* **117** 1202
[14] Park H W, Kim S B and Sohn H 2009 *Wave Motion* **46** 451
[15] Gangadharan R, Murthy C R L, Gopalakrishnan S and Bhat M R 2009 *Ultrasonics* **49** 696
[16] Xu B and Giurgiutiu V 2007 *J. Nondestruct. Eval.* **26** 123
[17] Sohn H, Park H W, Law K H and Farrar C R 2007 *J. Aerospace Engineering* **20** 141
[18] Park H W, Sohn H, Law K H and Farrar C R 2007 *J. Sound and Vibration* **302** 50
[19] Achenback J D 2003 *Reciprocity in Elastodynamics* (Cambridge: Cambridge University Press) p55